

GL-TR-90-0078

HIGH POWER OBLIQUE INCIDENCE HF
IONOSPHERIC MODIFICATION

AD-A224 402

Gary S. Sales
Ian G. Platt

University of Lowell
Center for Atmospheric Research
450 Aiken Street
Lowell, Massachusetts 01854

April 1990

Scientific Report No. 1

DTIC
ELECTE
JUL 31 1990
S E D

Approved for public release; distribution unlimited.

GEOPHYSICS LABORATORY
AIR FORCE SYSTEMS COMMAND
UNITED STATES AIR FORCE
HANSCOM AIR FORCE BASE, MA 01731-5000

"This technical report has been reviewed and is approved for publication"



JOHN L. HECKSCHER
Contract Manager



JOHN E. RASMUSSEN
Branch Chief

FOR THE COMMANDER



ROBERT A. SKRIVANEK
Division Director

This report has been reviewed by the ESD Public Affairs Office (PA) and is releasable to the National Technical Information Service (NTIS).

Qualified requestors may obtain additional copies from the Defense Technical Information Center. All others should apply to the National Technical Information Service.

If your address has changed, or if you wish to be removed from the mailing list, or if the addressee is no longer employed by your organization, please notify GL/IMA, Hanscom AFB, MA 01731. This will assist us in maintaining a current mailing list.

Do not return copies of this report unless contractual obligations or notices on a specific document require that it be returned.

REPORT DOCUMENTATION PAGE				Form Approved OMB No. 0704-0188	
1a. REPORT SECURITY CLASSIFICATION Unclassified		1b. RESTRICTIVE MARKINGS			
2a. SECURITY CLASSIFICATION AUTHORITY		3. DISTRIBUTION / AVAILABILITY OF REPORT Approved for public release; distribution unlimited.			
2b. DECLASSIFICATION / DOWNGRADING SCHEDULE					
4. PERFORMING ORGANIZATION REPORT NUMBER(S) UIRF-456/CAR		5. MONITORING ORGANIZATION REPORT NUMBER(S) GL-TR-90-0078			
6a. NAME OF PERFORMING ORGANIZATION University of Lowell		6b. OFFICE SYMBOL (if applicable)	7a. NAME OF MONITORING ORGANIZATION Geophysics Laboratory		
6c. ADDRESS (City, State, and ZIP Code) Center for Atmospheric Research 450 Aiken Street Lowell, Massachusetts 01854		7b. ADDRESS (City, State, and ZIP Code) Hanscom Air Force Base Massachusetts 01731-5000			
8a. NAME OF FUNDING / SPONSORING ORGANIZATION Geophysics Laboratory		8b. OFFICE SYMBOL (if applicable)	9. PROCUREMENT INSTRUMENT IDENTIFICATION NUMBER F19628-87-K-0012		
8c. ADDRESS (City, State, and ZIP Code) Hanscom Air Force Base Massachusetts 01731-5000		10. SOURCE OF FUNDING NUMBERS			
		PROGRAM ELEMENT NO. 61102F	PROJECT NO. ILIR	TASK NO. 7I	WORK UNIT ACCESSION NO. AA
11. TITLE (Include Security Classification) High Power Oblique Incidence HF Ionospheric Modification					
12. PERSONAL AUTHOR(S) Gary S. Sales; Ian G. Platt					
13a. TYPE OF REPORT Scientific No. 1		13b. TIME COVERED FROM 2/25/87 TO 2/25/88	14. DATE OF REPORT (Year, Month, Day) 1990 April		15. PAGE COUNT 46
16. SUPPLEMENTARY NOTATION					
17. COSATI CODES			18. SUBJECT TERMS (Continue on reverse if necessary and identify by block number) Ionosphere, Modification, HF, Interferometer, Ray Tracing, Doppler Shift, Arrival Angle, Signal to Noise		
FIELD	GROUP	SUB-GROUP			
19. ABSTRACT (Continue on reverse if necessary and identify by block number) In order to successfully perform the proposed ionospheric modification experiment (IONMOD) it is necessary to establish the range of the expected changes in the ionosphere, the parameters that offer the greatest likelihood of detection of these changes and the systems that can best carry out the appropriate measurements to detect them. The disturbed region of the ionosphere is modeled as a spherical depletion region of varying depth and size. Three dimensional numerical ray tracing is then used to determine the expected magnitude and location of the amplitude and arrival angle deviations. These calculations indicate rather small changes, of the order of 3 dB in amplitude and about 0.5° in the elevation angle, with even smaller changes in the azimuth arrival angle. This leads to strong requirements for the measuring system in terms of antenna design and the signal to noise that must be achieved. We also consider the basic concept of a probe system that can make the required amplitude and arrival angle measurements. Such a system will be based upon the real-time calculation of the Doppler spectrum of the signal on each antenna of the					
20. DISTRIBUTION / AVAILABILITY OF ABSTRACT <input checked="" type="checkbox"/> UNCLASSIFIED/UNLIMITED <input type="checkbox"/> SAME AS RPT <input type="checkbox"/> DTIC USERS			21. ABSTRACT SECURITY CLASSIFICATION Unclassified		
22a. NAME OF RESPONSIBLE INDIVIDUAL John Heckscher		22b. TELEPHONE (Include Area Code) 617-377-4052		22c. OFFICE SYMBOL GL/LID	

19. ABSTRACT

system and use the measured phase difference on each line in the spectrum, as an interferometer, to determine the arrival angle and amplitude. Finally with this concept in mind we set forth to determine the requirements for the signal to noise ratio that will permit the measurements with sufficient accuracy. The results indicate that sufficient measurement sensitivity of the probe system can be achieved with a transmitter power of 100 W continuous and an antenna pre-amplifier (with a low noise front end) properly designed to be atmospherically noise limited.

Accession For	
NTIS GRA&I	<input checked="" type="checkbox"/>
DTIC TAB	<input checked="" type="checkbox"/>
Unannounced	<input type="checkbox"/>
Justification	
By _____	
Distribution/	
Availability Codes	
Dist	Avail and/or Special
A-1	



TABLE OF CONTENTS

	Page
1.0 INTRODUCTION	1
2.0 GEOMETRY OF THE MODIFIED REGION	2
3.0 SIMULATION	8
3.1 Effect of the Depletion Level	8
3.2 Curvature Effects	12
3.3 Angle of Arrival	15
4.0 LOCATION OF THE RECEIVERS	19
5.0 FREQUENCY MANAGEMENT	22
6.0 BASIC HF PROBE SYSTEM	25
6.1 Measurements	27
6.1.1 Amplitude	27
6.1.2 Doppler Shift	28
6.1.3 Angle of Arrival	29
6.2 Calibration	29
6.3 Data Recording	30
7.0 HF PROBE SIGNAL TO NOISE RATIO REQUIREMENTS	31
7.1 Introduction	31
7.2 Signal to Noise Ratio Requirements	31

TABLE OF CONTENTS (Continued)

	Page
7.3 Signal to Noise Ratio Calculations	34
7.3.1 Received Signal Power	34
7.3.2 Noise	35
7.3.2.1 Atmospheric noise	35
7.3.2.2 Receiver noise	36
7.3.2.3 Heater transmitter leakage	36
7.3.3 Signal to Noise Calculation/System Margin	37
8.0 SUMMARY	38
9.0 REFERENCES	40

LIST OF FIGURES

Figure No.		Page
1	The two caustic regions produced by ray focusing within a nighttime ionosphere	3
2	Electron density profiles for the depleted region as given by equation 1	5
3	Alpha-Chapman layer used for the nighttime background ionosphere. $f_oF2 = 4$ MHz, $hmF2 = 330$ km.	7
4	Skip distances for operating frequencies of 9.7 MHz and 11.85 MHz	9
5	Variation of the probes received power for various percentage levels of depletion. $f_o = 9.7$ MHz. Depletion diameter = 100 km.	10
6	Variation of the probes received power for various percentage depletion levels. $f_o = 11.85$ MHz. Depletion diameter = 100 km.	11
7	Variation of the probes received power for various depletion diameters. $f_o = 9.7$ MHz. Depletion level = 5%.	13
8	Variation of the probes received power at various depletion levels for the two dimensional case. $f_o = 9.7$ MHz. Depletion diameter = 100 km.	14
9	Variation of the probes received vertical elevation angle for various depletion levels. $f_o = 9.7$ MHz. Depletion diameter = 100 km.	16
10	Deviation of the probes received vertical elevation angle from the 0% depletion model. $f_o = 9.7$ MHz. Depletion diameter = 100 km.	17

LIST OF FIGURES (Continued)

Figure No.		Page
11	Deviation of the probes received vertical angle of arrival from the 0% depletion model for various depletion diameters. $f_o = 9.7$ MHz. Depletion level = 5%.	18
12	The effect of including the earth's magnetic field on ground range values. NF = no field, O = ordinary, X = extraordinary. $f_o = 9.7$ MHz. Depletion diameter = 100 km.	20
13	Flow diagram for frequency management of the IONMOD experiment	23

1.0 INTRODUCTION

The proposed HF ionospheric modification experiment will use a high power radio beam from the VOA transmitting facility at Delano to heat the ionosphere in the vicinity of Albuquerque (NM) some 1200 km away. This obliquely heated region will be monitored via a low power channel probe system whose ray path passes through the heated region, and by a vertical incidence sounder near the midpoint at Albuquerque. The heater will obtain its high power from the three VOA 375 kW transmitters and new high gain 2-D antennas.

The channel probe system will have its transmitter collocated with the heater transmitter in Delano and a receiver at a site located at Barksdale AFB outside of Shreveport LA (2400 km from Delano).

A Digisonde 256 vertical incidence sounder, built and operated by the University of Lowell Center for Atmospheric Research (ULCAR), will be used to monitor the ionosphere near the midpoint of the path between Delano and Shreveport. The closest Air Force facility to the midpoint is the Kirtland AFB just outside Albuquerque.

It is the purpose of this report to estimate the effects of the heated region of the ionosphere on the probe signal and the receiver ranges most appropriate to maximize the detection of these effects. For a detailed description of the ionospheric heating process and possible resulting large scale structures see, for example, *Field and Warber (1985)*.

2.0 GEOMETRY OF THE MODIFIED REGION

The caustic surface generated by high powered oblique radio propagation can cause intense electric fields within the ionosphere. This may result in electron heating causing dynamic changes, modified recombination rates and diffusion rates as well as possible non-linear effects depending on wave power and location in the ionosphere, etc. [see for example *Gurevich, (1978)*]. For this particular study, only the F-region is considered, where the predominate heating effect is to cause a localized decrease in the electron density. A low power radio wave passing through this modified region will thus be deviated by its consequent change in the refractive index. The high power modifying wave also experiences a self action which can cause the depletion to vary non-linearly with time.

Since the approximations of geometric optics are invalid near regions of strong focusing, other methods for calculating the intensity of electric fields in the vicinity of the caustic must be used. Such a method, using a numerical integral extension to the standard ray tracing formulas, was developed by *Warren, De Witt and Warber (1982)* and used by *Field and Warber (1985)* to calculate the focused field intensities and consequent heat energy input to the F-region. They showed, for a night time ionosphere, that the resulting depletion may be up to 100 km in size with a location near the branch point of the two caustic surfaces (see Figure 1). Since diffusion within the depleted region has only been approximated, however, the extent of the percentage electron depletion is still somewhat in question. For this reason when it becomes necessary to estimate the percentage of ionospheric modification, values of 1%, 5% and 10% are taken as representative. The actual shape of the depleted region is also unknown and for the simulation presented here we have assumed that it is spherically shaped. This provides a simple form of graded surface for studying many of the general effects due to geometry. Certainly major characteristics such as the cross-sectional curvature perpendicular to the ray path can be well represented by a sphere. The electron density distribution function N_c of such a depletion is given by:

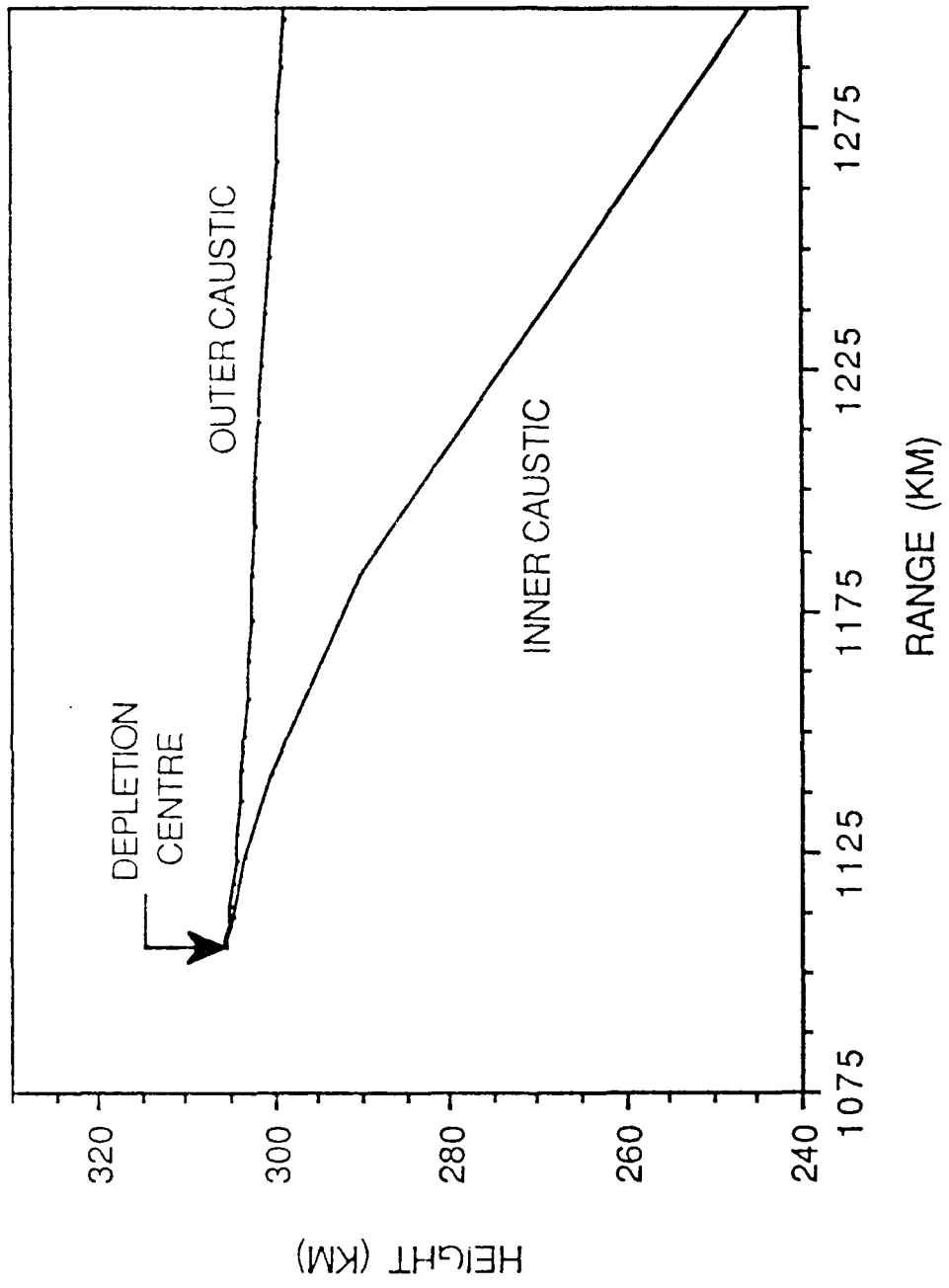


Figure 1. The two caustic regions produced by ray focusing within a nighttime ionosphere

$$N_C = N_B \left(1 - \frac{A}{1 + R^M} \right) \quad (1)$$

Where

N_B = Background nighttime ionosphere (Alpha Chapman Layer)

M = Power controlling the shape of the walls electron density profile

A = Depletion level (e.g. $A = 0.01$ equal to one percent)

and

$$R = \frac{\left[(x_0 - x)^2 + (y_0 - y)^2 + (z_0 - z)^2 \right]}{a^2}$$

where

(x_0, y_0, z_0) = Cartesian Coords. of the depletion center

(x, y, z) = Cartesian coords. of the ray

and a = half width radius of the sphere.

This electron density distribution function is included in the ray tracing program via its derivatives with respect to the computational coordinate system (i.e. spherical). Figure 2 shows the cross-sectional electron density profiles of the spherical hole relative to the background ionosphere, for several different values of the parameter M .

The proposed IONMOD experiments are to be conducted during the night since at these times the heating is predicted to be more pronounced. For the background ionosphere, at these times, a single alpha-Chapman layer is used. This is a convenient model when using numerical ray tracing, since it avoids matching base and peak layer heights and easily facilitates the

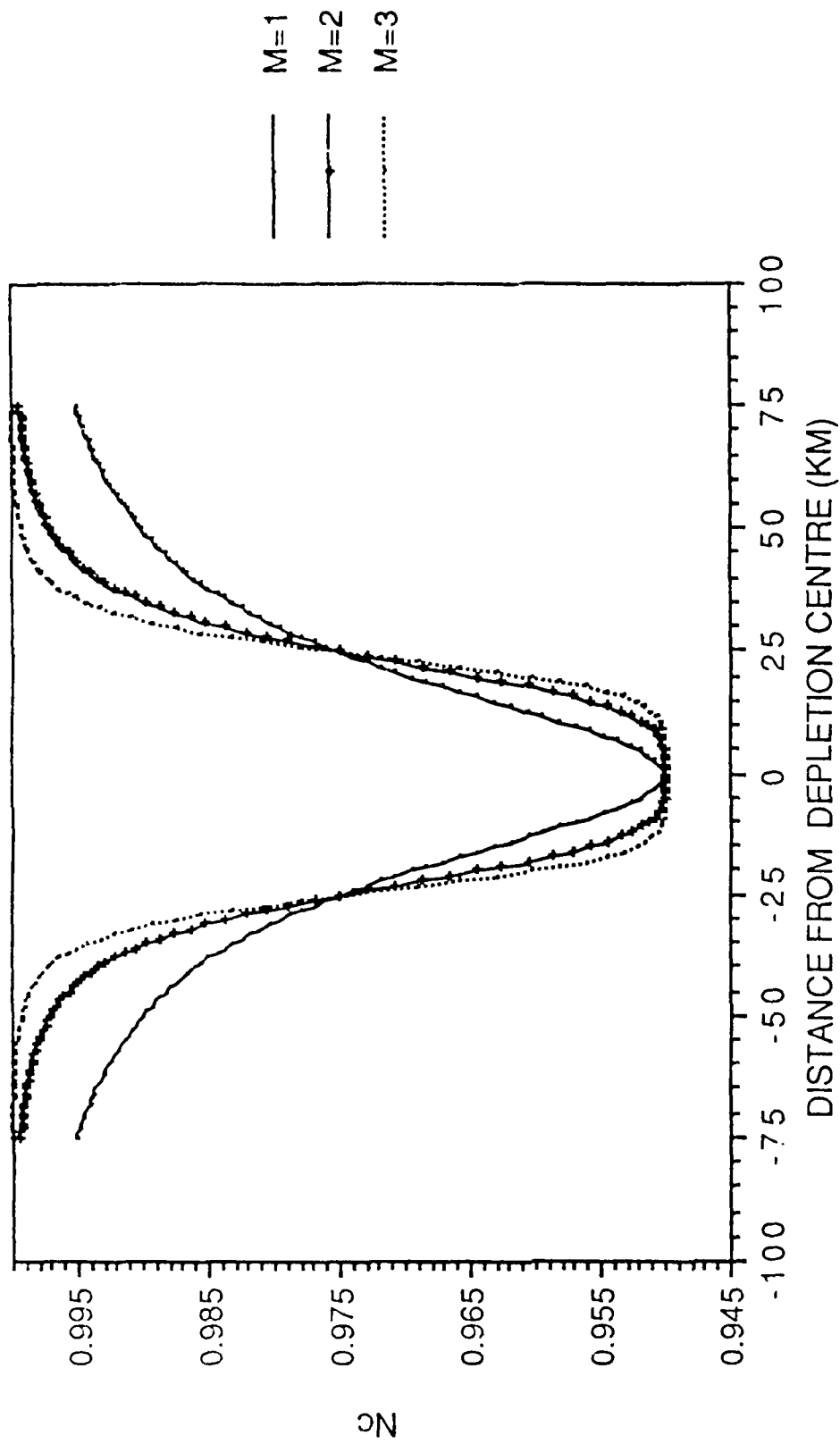


Figure 2. Electron density profiles for the depleted region as given by equation 1

inclusion of horizontal gradients. An example of a profile used for the night time calculations is shown in Figure 3.

Ray tracing on a large scale, using the Jones-Stephenson [1975] program, was carried out through the above mentioned depleted region immersed in a background nighttime ionosphere to determine power, range and elevation angle variation during the heating experiment. For most cases the earth's magnetic field is ignored. Received power is calculated from the cross product of three closely spaced rays, so that unless otherwise stated the measurements are three dimensional. Power measurements are given in terms of path loss in decibels.

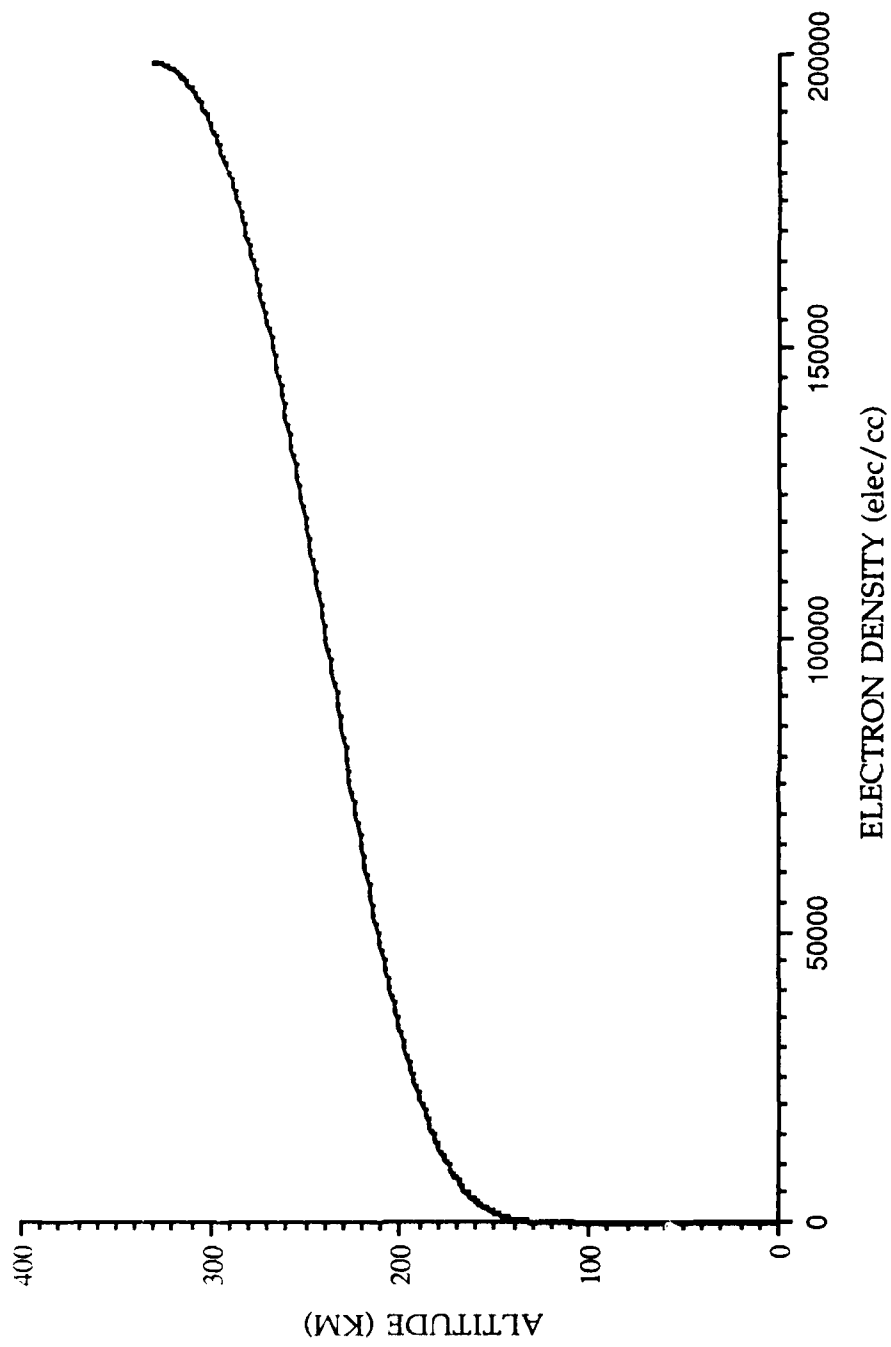


Figure 3. Alpha-Chapman layer used for the nighttime background ionosphere. foF2 = 4 MHz, hmF2 = 330 km

3.0 SIMULATION

3.1 Effect of the Depletion Level

Using a 100 km diameter depletion, ray tracing was carried out for foF2 values of 4 MHz and 5 MHz with hmF2 = 330 km. To maintain the skip at a relatively constant range requires a corresponding oblique operating frequency change of 9.7 MHz and 11.85 MHz (see Figure 4 for the two foF2 values). The received power for both cases is shown in Figures 5 and 6 for the three values of percentage depletion. Both figures show that for all depletions there is a region of increased received power followed by a smaller region at longer ranges of decreased power reception.

Two conclusions can be drawn. For each operating frequency the cross-over point between the gain and loss regions is similar for all the depletion levels and secondly, for a constant heated region diameter, an increase in depletion level always results in an increased variation of received power. While the range dependence of the power variation for the two operating frequencies is similar, the effective range of increased power is decreased by about 50 km for the fo = 11.85 MHz case and this changes the optimal reception distance from Delano.

Figures 5 and 6 also show that for a small depletion level of 1%, the power changes become extremely small (less than 0.5 dB). Changes in power due to heated regions of high curvature and low depletion level will therefore be difficult to observe. This situation will be altered when the physical size (and thus also curvature) of the depletion is changed and this is discussed in more detail below.

Self action of the heater beam was neglected in all cases studied here.

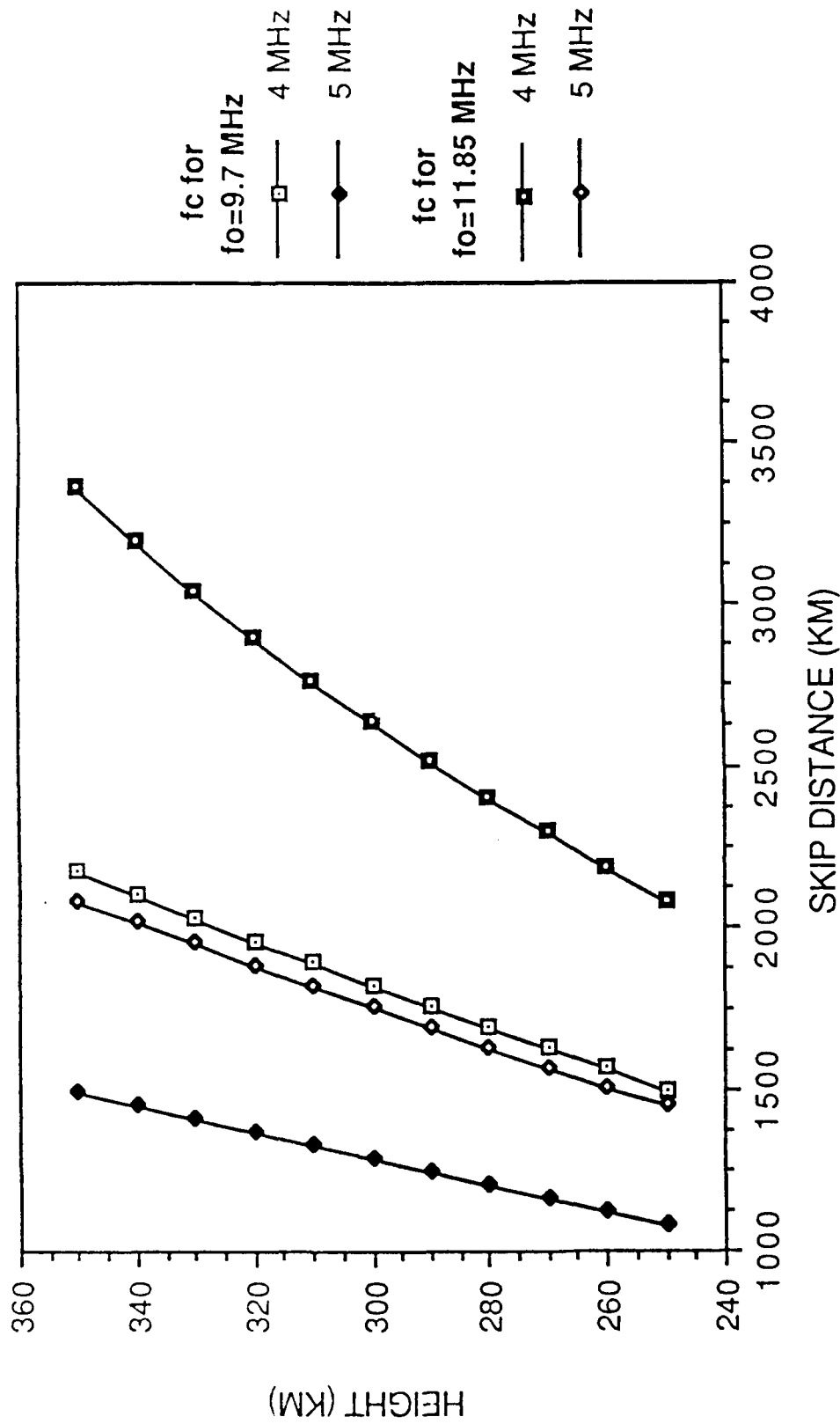


Figure 4. Skip distances for operating frequencies of 9.7 MHz and 11.85 MHz

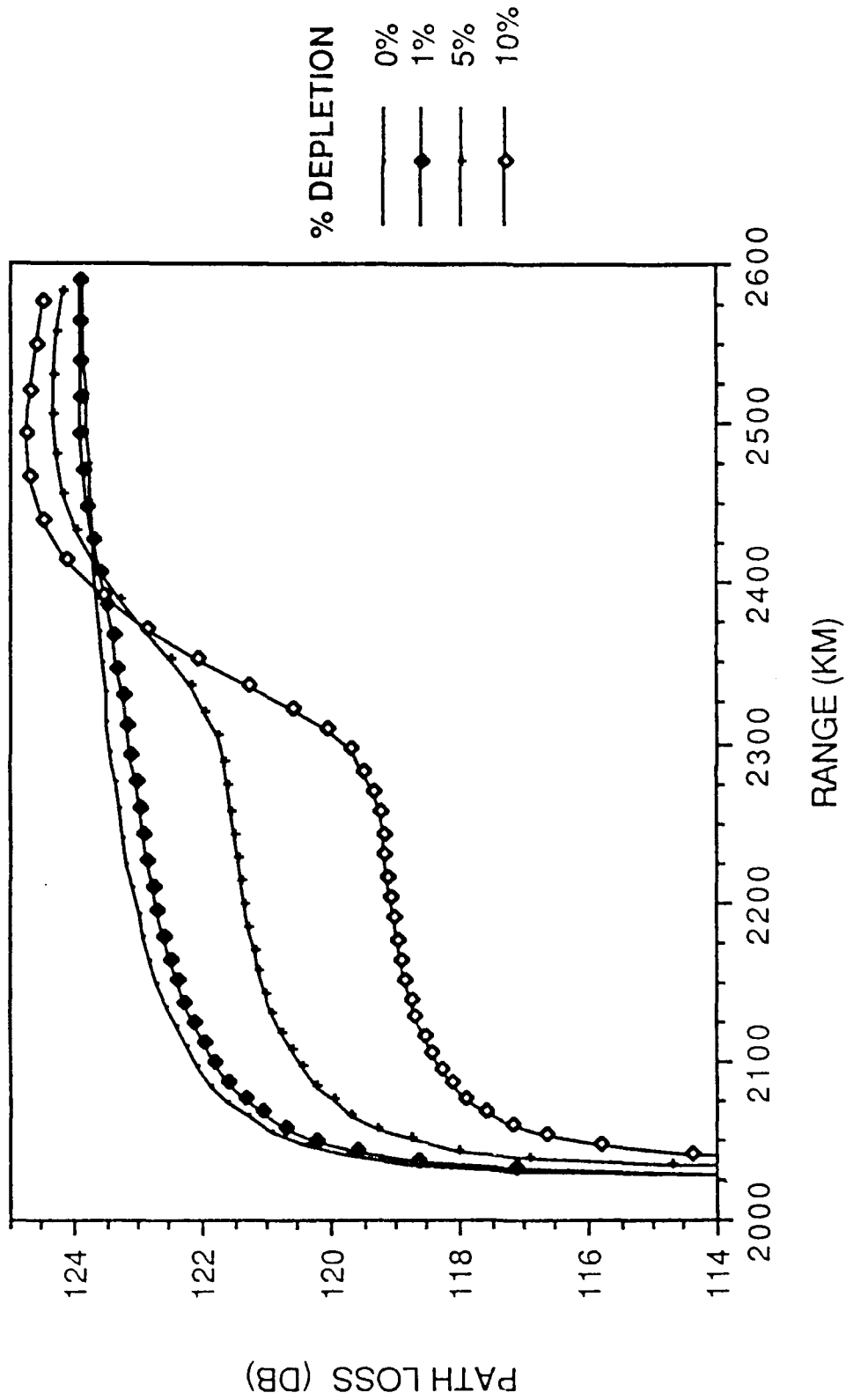


Figure 5. Variation of the probes received power for various percentage levels of depletion. $f_0 = 9.7$ MHz. Depletion diameter = 100 km.

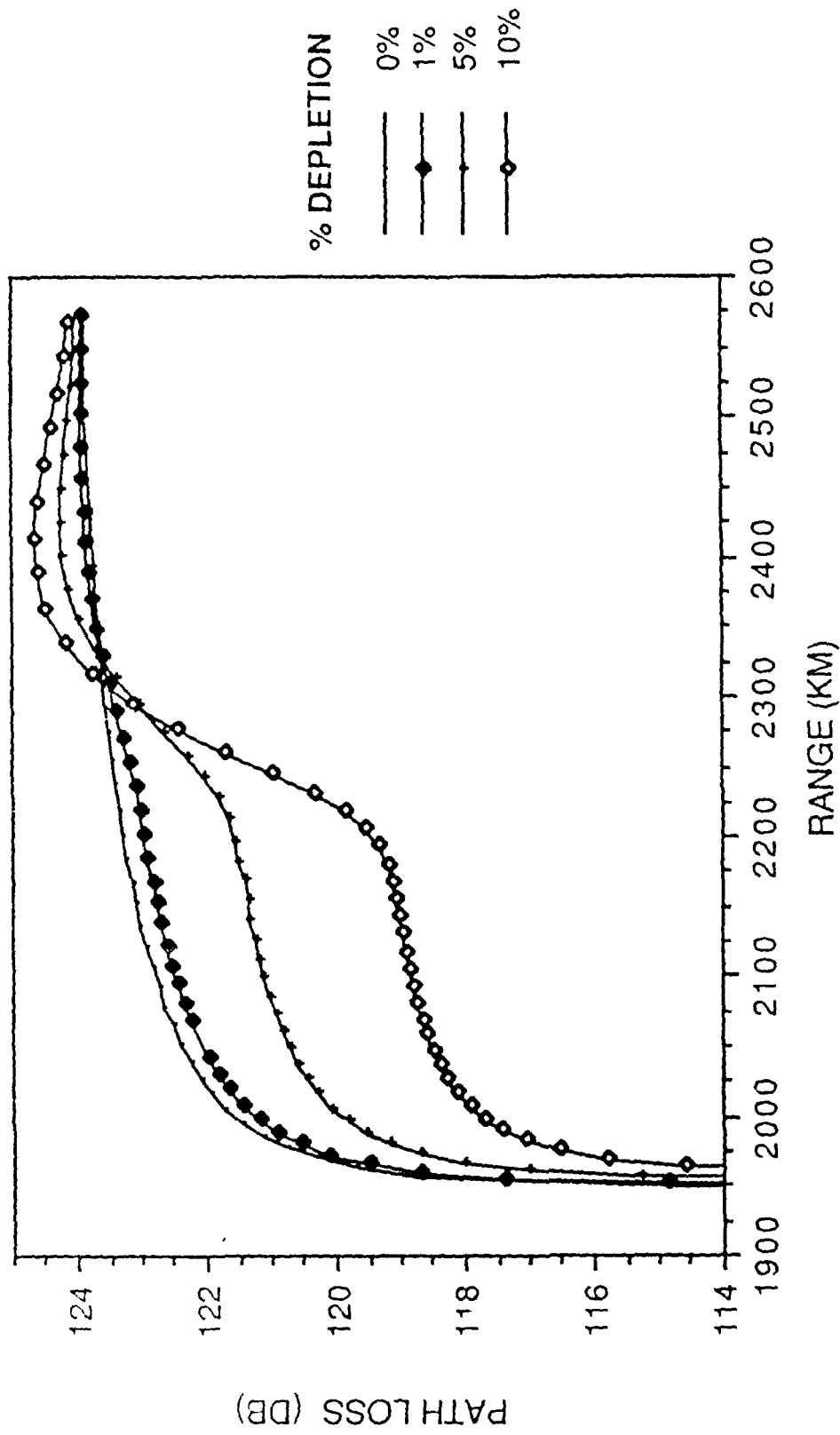


Figure 6. Variation of the probes received power for various percentage depletion levels. $f_o = 11.85$ MHz. Depletion diameter = 100 km.

3.2 Curvature Effects

The cross-sectional curvature of the depleted region has a considerable effect on beam focusing and thus received power. This can be seen clearly in Figure 7, where the received power is plotted for various depletion diameters. Here the plot is for a ray path within the vertical plane containing the transmitter point and center of the disturbance. For diameters above approximately 12 km focusing occurs thus causing increased power, while for diameters less than 12 km strong defocusing can occur accompanied by a decrease in received power. This sort of effect is typical of three dimensional structures acting as lenses, and though difficult to show for the graded refractive index profile is easily seen by a simple analogy with a more abrupt profile [see *Born and Wolf* (1964)]. In the examples given here it is the cross-sectional curvature perpendicular to the plane containing the ray path that has the most effect on curvature focusing (i.e. azimuthal rays focus more strongly). The amount of focusing due to the azimuthal rays can be demonstrated by comparing the 2-D case in Figure 8 with the previous 3-D case of Figure 7. For the 2-D example only two rays of closely spaced elevation are used for the power calculations. For this case power variations are extremely small even with a 5% depletion. Here the received power increases with the diameter, since the predominant effect of azimuthal focusing is not included.

Clearly the cross-sectional shape of the depletion region is of vital importance in assessing the success of observing power variations due to ionospheric modification. Three major factors influencing the depletion shape and thus the sensitivity of the planned experiment are:

1. Antenna radiation pattern.
2. Caustic shape produced by ionospheric conditions.
3. Non-linear diffusion effects.

Since at this stage there is little knowledge about points 2 and 3, they must be considered as unknown factors.

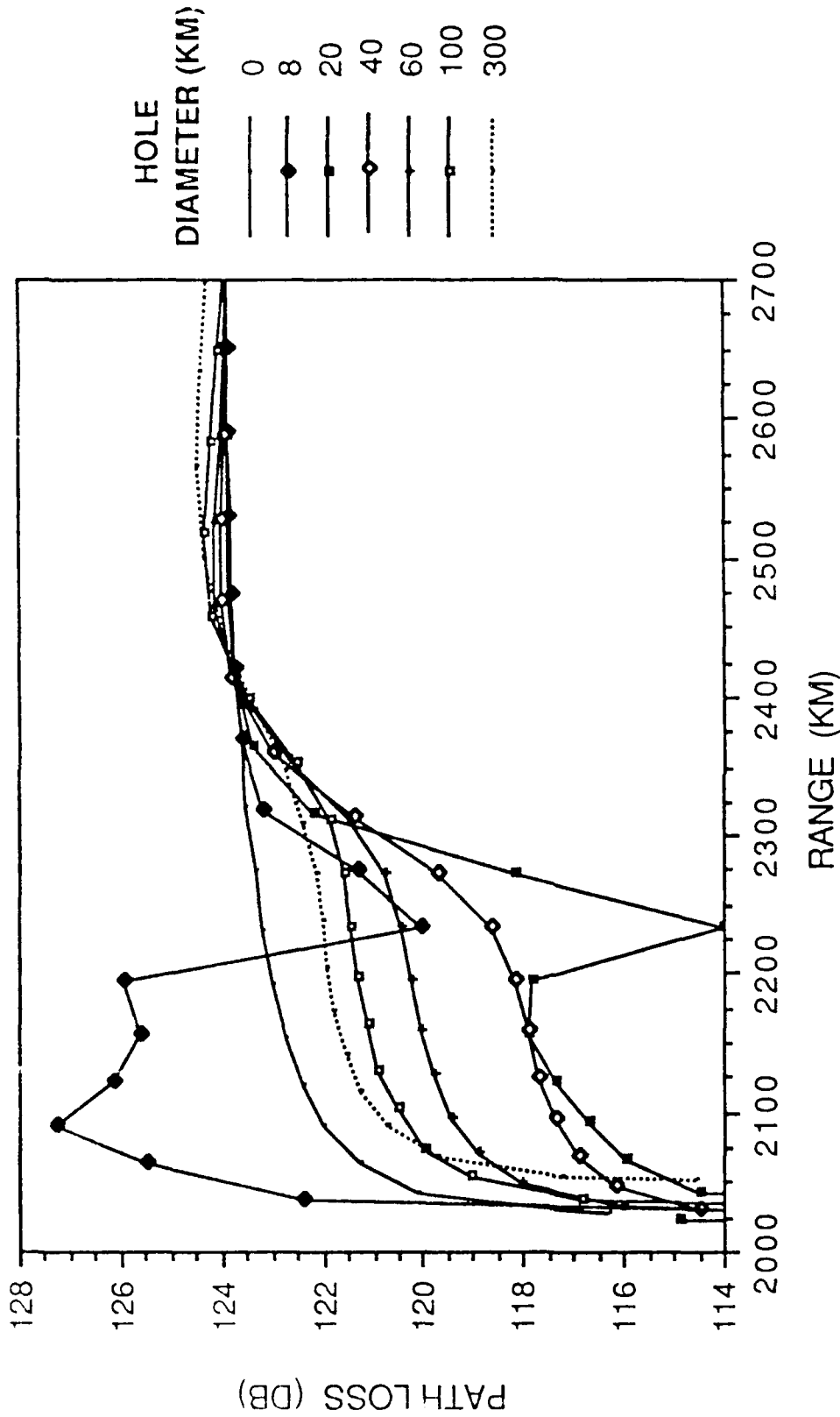


Figure 7. Variation of the probes received power for various depletion diameters. $f_0 = 9.7$ MHz. Depletion level = 5%.

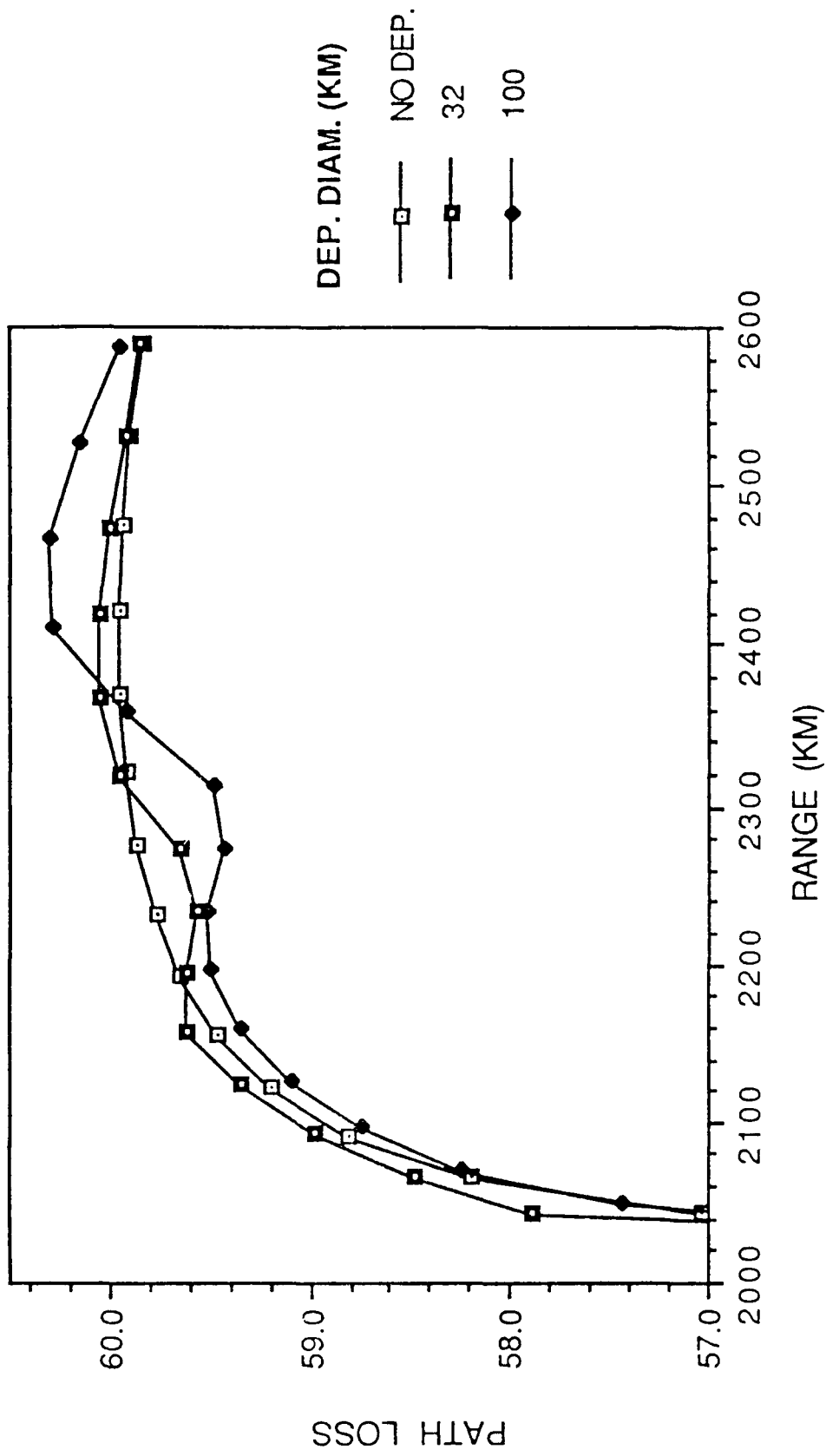


Figure 8. Variation of the probes received power at various depletion levels for the two dimensional case. $f_0 = 9.7$ MHz. Depletion diameter = 100 km.

3.3 Angle of Arrival

The elevation angle of arrival variation for various percentage depletions is shown in Figure 9. Figure 10 gives the angle of arrival deviation from the zero depletion case. It is clear from Figure 10 that as the percentage depletion increases the deviation also increases. From Figures 5 and 6 it can be seen that the largest power variations occur at a range of 0 to approximately 300-350 km from the skip. For the angles of arrival, however, Figure 10 shows that this is the region of smallest deviation. In this region, depletions between 0-5% give such small variations in the angle of arrival that detection of the heated region by this means appears to be doubtful. Figure 11 shows that as the depletion diameter is increased the variation in elevation angle is always increased. This means that the curvature for optimizing angle of arrival variations does not correspond to that required for optimizing power variations.

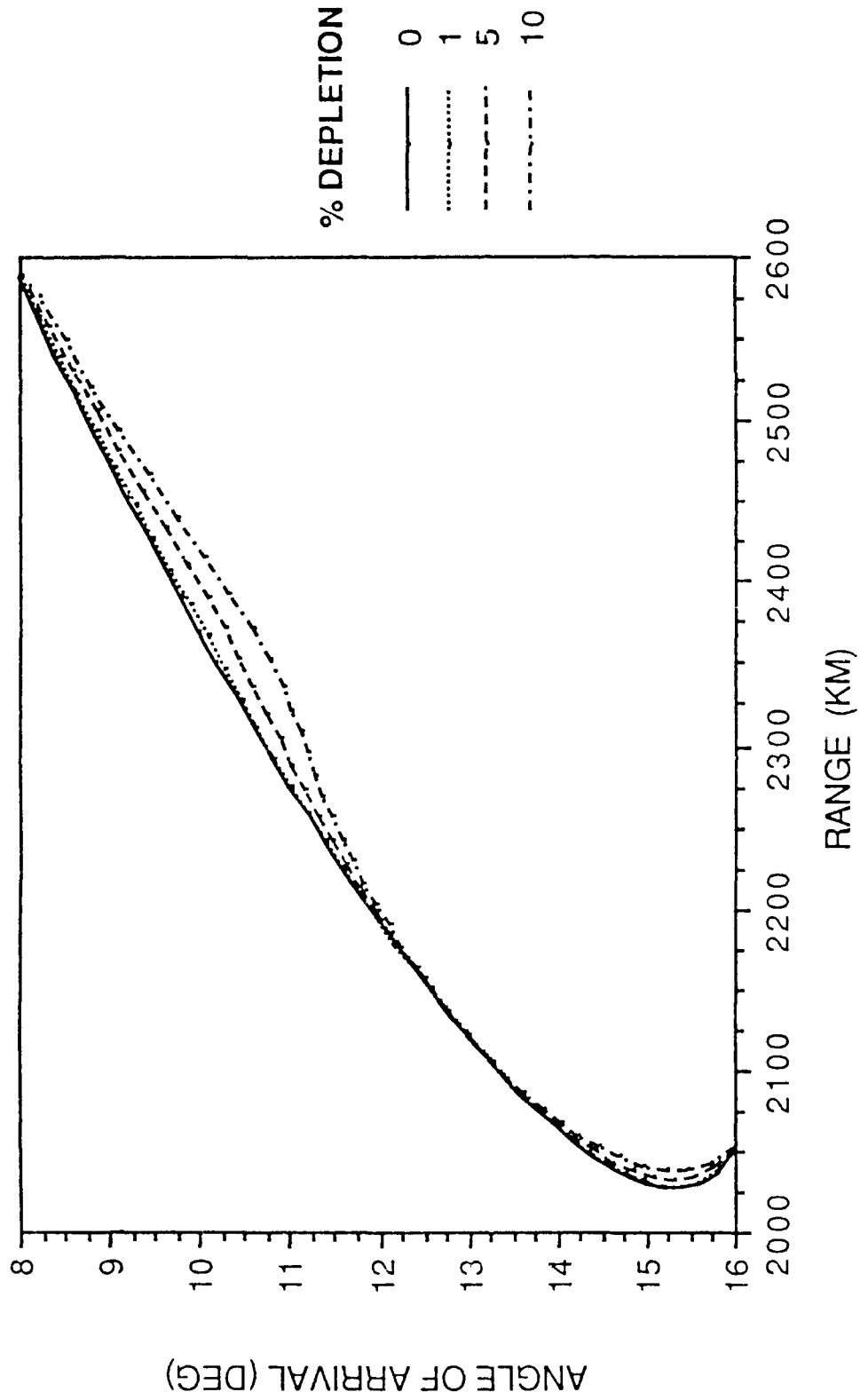


Figure 9. Variation of the probes received vertical elevation angle for various depletion levels. $f_0 = 9.7$ MHz. Depletion diameter = 100 km.

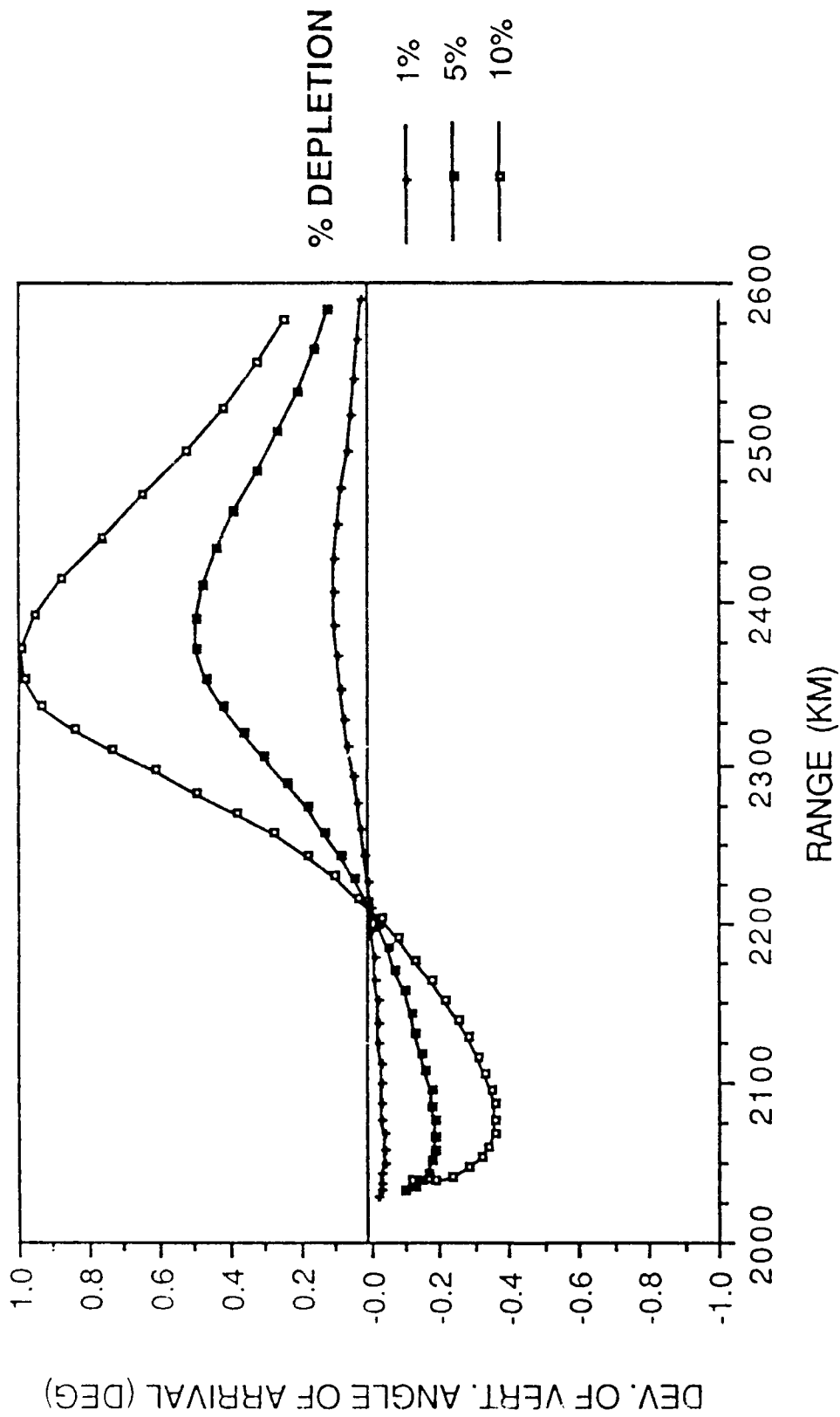


Figure 10. Deviation of the probes received vertical elevation angle from the 0% depletion model. $f_0 = 9.7$ MHz. Depletion diameter = 100 km.

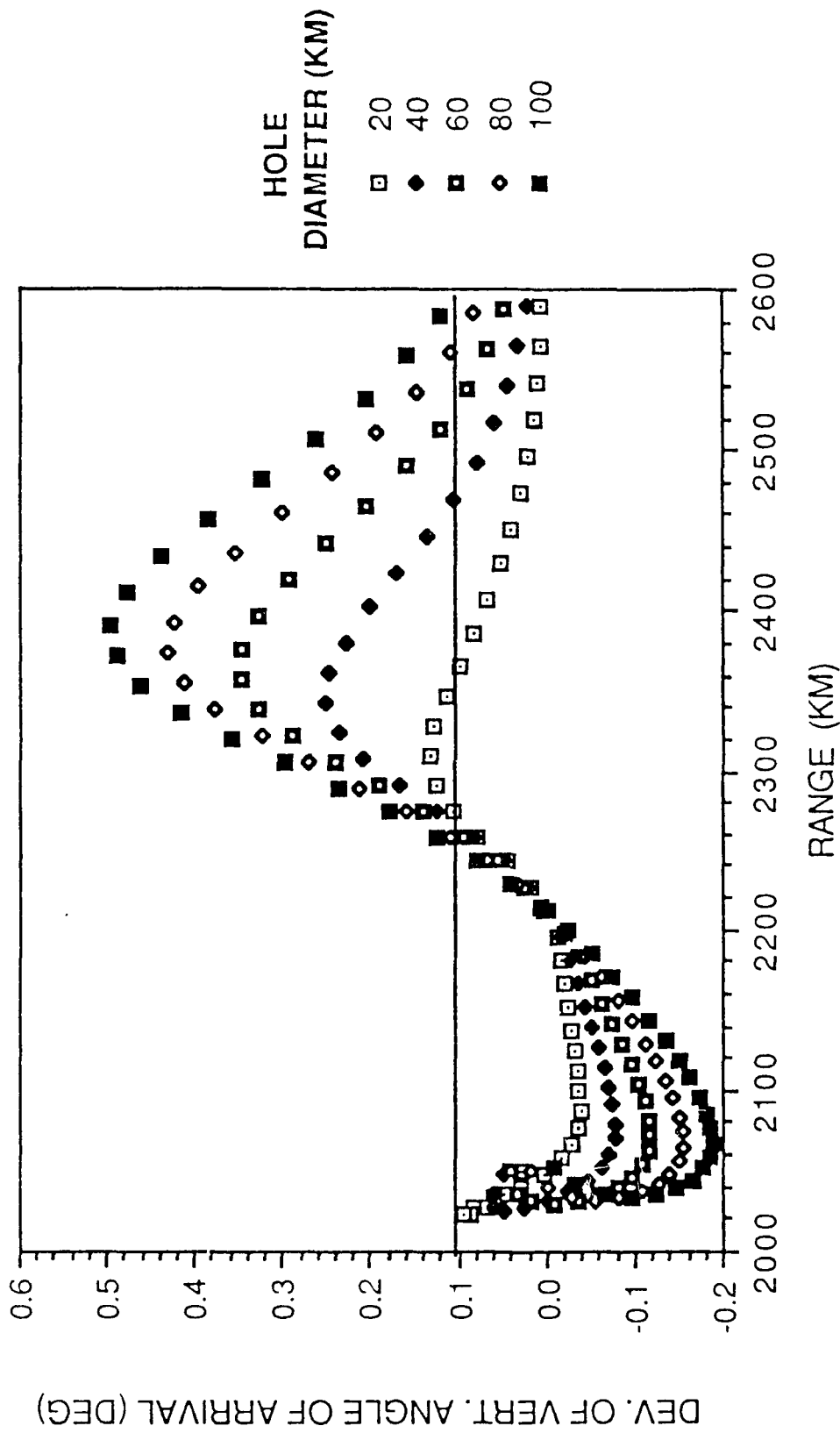


Figure 11. Deviation of the probes received vertical angle of arrival from the 0% depletion model for various depletion diameters. $f_0 = 9.7$ MHz. Depletion level = 5%.

10. LOCATION OF THE RECEIVERS

From the power plots of Figures 5 to 7 it is clear that the maximum power variation is located near the skip. However, changes in the shape and level of the depletion can vary the skip distance over a range of about 15 km. The inclusion of the magnetic field causes the skip distance of the ordinary mode to be increased by approximately 20 km from the no-field case, while the skip distance for the extraordinary mode is decreased by approximately 50 km from the no field case (see Figure 12). The azimuthal variation caused by the magnetic field is minimal. From Figures 5 to 7 it can be seen that for most depletions and cross sections, a cross-over point between increased and decreased power from the background ionosphere occurs between 350-375 km from the skip. However, the variation in received power decreases rapidly, approximately 50 km before this cross-over point. Combining the uncertainties due to inclusion of the magnetic field and the exact position of the cross-over point would give an optimal range window for power variation between 50-300 km from the skip.

The optimal range position for maximum power and vertical angle of arrival variations do not overlap. Depending on the estimated depletion level and size, background noise, etc., angle of arrival variations may be more easily distinguished than power variations. This would require an extra receiver in the range 300-450 km from the skip.

The major points affecting the success of the IONMOD experiment resulting from this work may be summarized as follows:

1. If the percentage depletion is small, both power and angle of arrival variations can be small (depending on depletion diameter). This would make changes in the probe signal hard to detect. At this stage we have not fully investigated the effect the heated region has on Doppler spread.

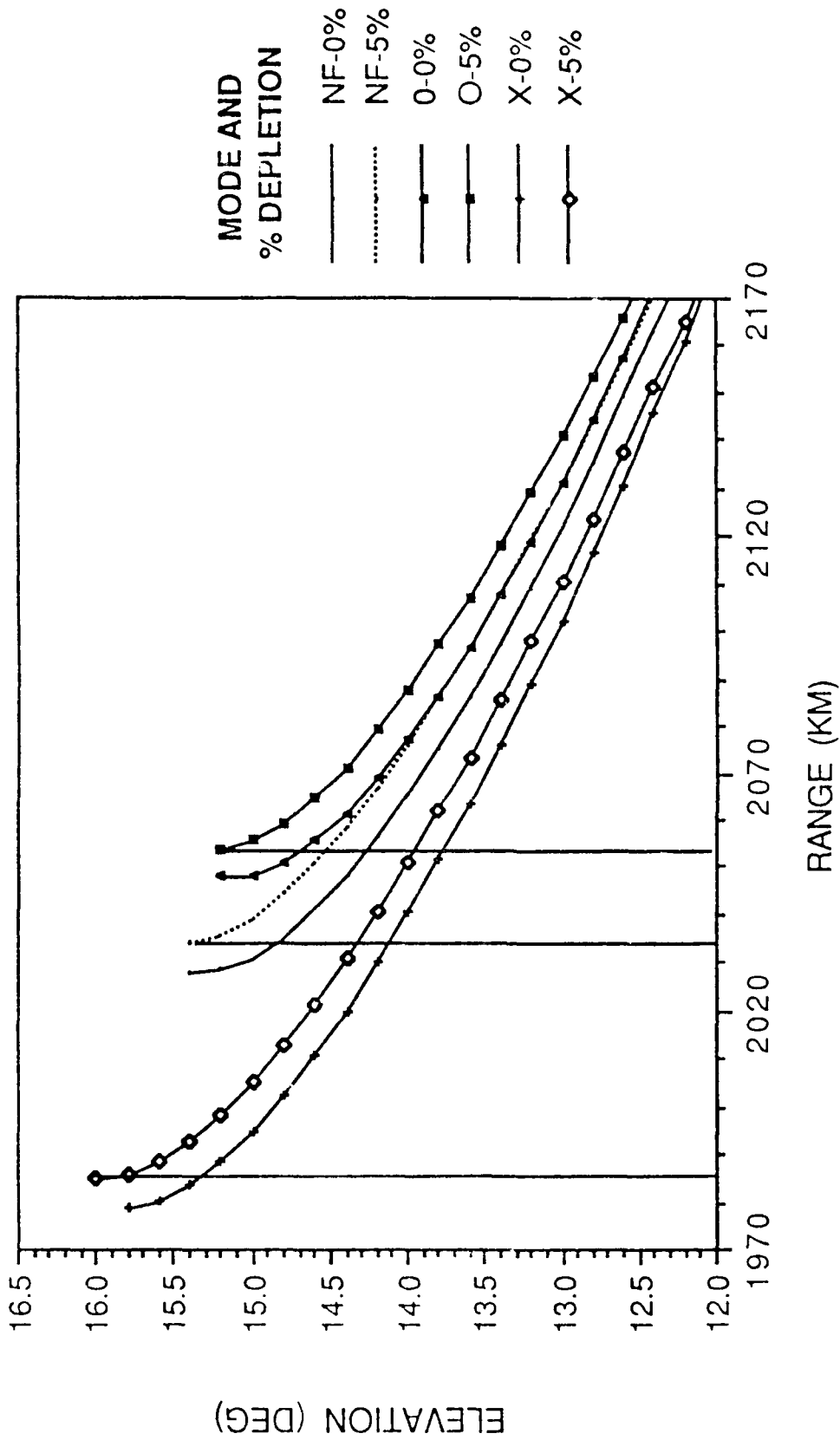


Figure 12. The effect of including the earth's magnetic field on ground range values. NF = no field, O = ordinary, X = extraordinary. $f_o = 9.7$ MHz. Depletion diameter = 100 km.

2. The shape of the depleted region is an important factor in determining received power. If the percentage depletion is small, a decrease in diameter could actually increase focusing sufficiently to enable observable power variations. The above points indicate that a reasonable estimate of both depletion level and size should be made as part of the experimental planning.
3. The optimal range for power variation remains fairly stable for changes in both depletion diameter and percentage electron density. This optimal range for power fluctuation is 50-300 km from the skip. It also seems important to place an extra receiver in the range 300-450 km from the skip, to detect angle of arrival variations.

5.0 FREQUENCY MANAGEMENT

The proposed operation for frequency and elevation angle management of the IONMOD experiment is shown in Figure 13. Real time ray tracing occurs in two phases:

1. Correction for Horizontal Gradients:

At this stage it is unlikely that real time estimates of the horizontal gradients can be made solely by Digisonde processing at the mid-point. An automatic adjustment for their inclusion is proposed by matching measured vertical angle of arrivals with those deduced by ray tracing. Estimates of the horizontal gradients will be periodically updated to allow for the effect of fluctuations due to gravity waves, etc. The midpoint sounder at Kirtland AFB (NM) will be used as a control point for gradient adjustment.

2. Frequency Correction for Operating Range:

From the previous sections it is clear that the optimal operating range is between 50-300 km from the skip. After the ionospheric model has been corrected for gradients, the skip distance is located by ray tracing and an operating frequency chosen which allows the receiver to remain within this optimal range. If an oblique sounder, operating between Delano and Shreveport were available, it could be used to improve model estimates of the plasma profile along the propagation path.

Numerical ray tracing programs may be used, but are slow and would thus require careful consideration for each project to minimize run time. Analytic programs, such as *La Bahns* (1987) complete with multiple layers are sufficiently accurate enough for most cases and extremely fast. This would not only facilitate a good real time frequency management tool, but also make practical the simulation of data requiring a large amount of ray

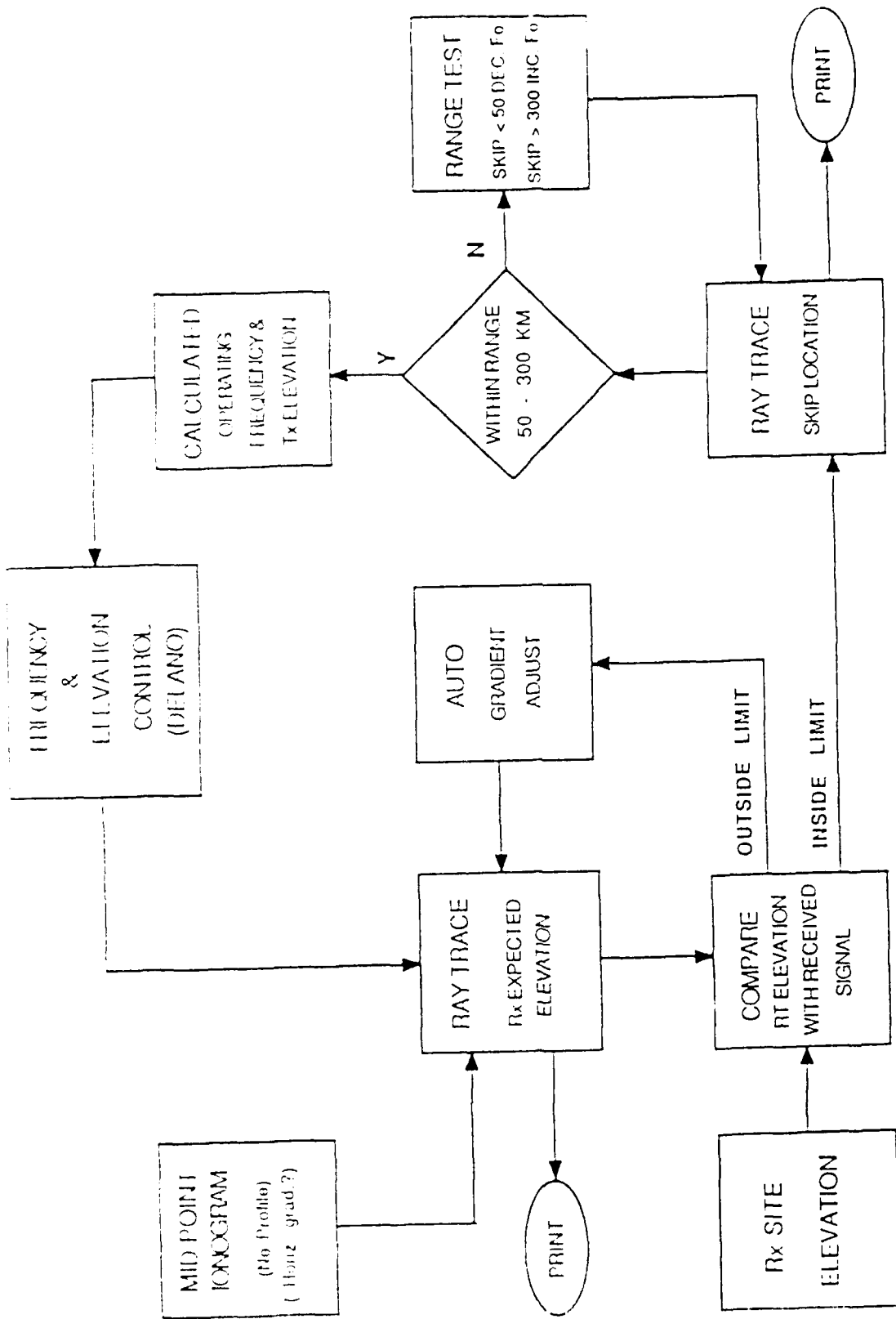


Figure 13. Flow diagram for frequency management of the IONMOD experiment

tracing. For future experiments and data analysis there is a definite requirement to develop a general form of analytic ray tracing.

6.0 BASIC HF PROBE SYSTEM

By employing a spatially diverse antenna array and modern signal processing, the channel probe system can be used to measure the following characteristics of the propagation path:

- (1) Amplitude variations - due to absorption, spatial defocusing, defocusing by plasma irregularities (these irregularities include plasma instabilities caused by the heating), scatter from irregularities.
- (2) Doppler Shift - due to motion and growth of irregularities and/or macroscopic changes in the ionosphere.
- (3) Angle of Arrival - vertical and horizontal angle of arrival. Measures deviations due to path modification by irregularities, changes in the macroscopic ionosphere and different propagation modes.
- (4) Multipath - Determination of multipath modes from angle of arrival and delay spread measurements.

The channel probe system will use a 150 W transmitter. The transmitter will be a solid state device located at the VOA field site in Delano, CA. The transmitting antenna for the probe system will be a sloping-V antenna mounted on a 30 m pole and covering the frequency range from 6 to 30 MHz. Ray tracing using IONCAP ionospheric models has shown that typical take-off angles of the order of 10° will be required for the selected path. The antenna design will provide for the expected take-off angles and element lengths of 130 m to 200 m will be necessary.

The transmitted signal will be a simple CW emission with proper identification periodically applied to the signal. The operating frequency will be determined using the VI Digisonde near the midpoint in New Mexico. The frequency information will be telephonically transmitted

from the sounder to the transmitter site at Delano, CA and to the receive site at Barksdale AFB.

The probe receiver system will consist of four antennas and four receivers (three receivers and antennas for the probe system and one receiver and antenna to directly monitor the VOA heater signal) connected to a Zenith Z-248 computer through an A/D convertor. The receiving antenna will be relatively simple, consisting of short active whips which operate over a wide range of frequencies and provide adequate signal and external noise to overcome the noisy front end of the RACAL receiver. Each of the antennas will be connected to a RACAL receiver and then interfaced with the Zenith computer. All of the basic signal processing will be done in real-time on the site computer. In addition to data compression, this processing will provide real-time monitoring that will enable the operators to check on system performance and on the character of the propagation effects.

In order to keep the total amount of data and processing time to a reasonable level, the received signal will be band limited using a narrow 150 Hz filter in the RACAL receiver. Since the experiment will be conducted in a mid-latitude region, Doppler fluctuations induced by the natural ionosphere and/or the heated ionosphere will usually be less than 10 Hz. Thus only Doppler information at 10 Hz around the center bandwidth will be retained, thus greatly reducing the on-site storage requirements. This processing includes Fourier analysis of the data from each receiver to obtain high resolution spectra making it possible to see the fine structure of the probe signal after it passes through the ionospherically disturbed region.

These probe transmissions will be made on a frequency selected by the midpoint monitoring system and can be set to any frequency within the HF band consistent with licensing for the Delano site. The separation will be adjusted to keep the very powerful heater transmitter out of the filter bandwidth of the probe receiver. The probe system will transmit continuously during the cycling of the heater transmitter.

6.1 Measurements

To maximize the potential for success, three basic measurements have been identified that should be made during the first phases of these experiments. These are:

- Amplitude
- Doppler frequency shift
- Vertical angle of arrival.

6.1.1 Amplitude

The formation of a heated region will likely be an area with reduced electron density that will tend to defocus and scatter the radio waves passing through it. The previous modeling has shown that the focusing and defocusing of the probe wave as it passes through the heated region may cause amplitude variations from +3 dB to -10 dB. Soviet measurements indicated expected changes of the order of 3 dB after the heater is turned on.

As will be shown later, accurate measurements require the transmitter to have sufficient power to provide a signal above noise of about 30 dB. This minimum SNR must be maintained over the above range of expected amplitude variations.

This should not be a problem if we can find clear channels in which to operate the probe experiment. Clear channels can be identified with a dedicated spectrum analyzer or with the RACAL receivers themselves. Signal to noise calculations (discussed below) confirm these expected levels and the Fourier processing will add some 30 dB more to the expected SNR.

The amplitude processing should have a high resolution capability since the previous simulations show that amplitude variations

may be small. At present a resolution of 0.009-0.280 dB (at a SNR of 60-30 dB respectively) is expected and this is well within the requirements.

The highest fading rates will likely be of the order of the fast fading that normally occurs on an HF path, i.e. 1 to 10 Hz. It is essential to spectrally analyze the data from each of these receive systems to separate the mode structure before computing the signal amplitude, since the different propagation modes (e.g. E, F, high, low rays, etc.) will have different paths through the ionosphere. This will reduce intermodal fading and it will thus be possible to recognize the effects of the heating on the particular mode passing through the disturbed region. For the amplitude measurements we would then combine the signal from the several antennas after spectrum processing to achieve the maximum processing gain.

6.1.2 Doppler Shift

The Fourier processing discussed above, directly yields the Doppler spectrum associated with each mode. A resolution of 0.05 Hz is sufficient to separate most forward scatter modes. Simulation has shown that forward propagation modes result in small Doppler shifts possibly less than 2 Hz. Since Doppler shifts will be small we must integrate for a relatively long time, say 10 or 20 seconds. This will give us frequency resolutions of 0.1 to 0.05 Hz respectively.

With the available signal processing in the computer, the spectrum analysis can be done in real-time. Using the 150 Hz filter, a sampling rate of 250 per second (complex) will be sufficient to insure that no aliasing occurs. For a 20 second integration, a 4096 point DFT will be carried out and then a selected band of frequencies (± 10 Hz) within the ± 125 Hz processing bandpass will be recorded. This integration time could be shortened if a higher time resolution is found to be necessary.

The possibility of designing a higher Doppler resolution mode into the processing system to permit recognition of the Doppler spread

scattering modes generated by irregularity formation in the heated region, is being evaluated. This mode would have to integrate for 80 secs. and require a 16,000 point DFT.

6.1.3 Angle of Arrival

A three antenna/receiver configuration will be used to measure the horizontal and vertical angles of arrival. This requires a simple L shaped antenna configuration. In order to determine the optimum separation between these antennas, preliminary calculations in terms of the expected range of elevation and azimuth angles are currently being carried out. It is expected that an antenna separation of the order of several wavelengths will satisfy the accuracy requirements determined from the simulations (Figure 10). With increased antenna spacing the phase difference and therefore the arrival angle measurement becomes more accurate for a given signal to noise ratio. On the other hand, the wider spacing decreases the unambiguous range of angles.

6.2 Calibration

Using three separate receivers, each with phase locked loops, it is likely that phase differences between the receivers will occur even though the same reference oscillator is used for them all. To avoid errors caused by these phase differences (internal to the receivers), a calibration system will be used to inject the same external reference signal into all the receivers. This calibration will be done before and after each change in operating frequency and processed and recorded in the same way as the probe signal.

6.3 Data Recording

Assuming the normal data taking mode is 10 or 20 seconds, then about 1.6×10^6 data points per antenna will be recorded during a six hour campaign. This data will be stored on the internal hard disk of the site computer. At the completion of the mission this data will be transferred to floppy disks and stored for future processing on any Zenith or IBM compatible computer.

7.0 HF PROBE SIGNAL TO NOISE RATIO REQUIREMENTS

7.1 Introduction

In order to accurately measure the expected small changes in amplitude, frequency and angle of arrival of the probe signal a rather high signal to noise ratio (SNR) at the probe receiving site is required. The angle of arrival changes calculated in this report (Figures 9 and 10) and as also measured by *Bochkarev* (1982) are of the order of 1° or less. The interferometer array, as part of the HF Probe System, uses three receiving antennas and measures the phase difference between the azimuth measuring pair of antennas and the phase difference between the vertical angle measuring pair (one antenna is in common between these two pairs of antennas). These interferometer measurements require SNR's of the order of 30 dB to achieve the necessary angle accuracy as will be shown below. The design of the probe system must be tailored to achieve these signal levels.

7.2 Signal to Noise Ratio Requirements

The SNR required to achieve the necessary accuracy to measure the angles of arrival using the phase difference method is calculated as follows:

The measured phase difference ϕ is given in terms of the wavelength, λ , antenna spacing, d , and the angle of arrival, θ , measured from the line perpendicular to the antenna baseline as:

$$\phi = \frac{2\pi d}{\lambda} \sin \theta \quad (1)$$

Assuming no uncertainty in the values of λ and d , it is possible to obtain an expression that describes the relationship between the expected change in the arrival angle θ in terms of the uncertainty in measured phase difference ϕ as (without solving for $\Delta\theta$ explicitly):

$$\Delta\phi = \frac{2\pi d}{\lambda} \cos \theta (\Delta\theta) \quad (2)$$

The phase measurement is made using the quadrature amplitude measurements I and Q as follows:

$$\phi = \arctan \left[\frac{I}{Q} \right] \quad (3)$$

The change or error in phase difference can then be related to the errors in the measurement in I and Q by differentiating Equation 3. This gives a second expression for $\Delta\phi$:

$$\Delta\phi = \frac{IQ}{(I^2 + Q^2)} \left[\frac{\Delta I}{I} - \frac{\Delta Q}{Q} \right] \quad (4)$$

Squaring equation (2) and equation (4) and setting them equal to each other gives:

$$(\Delta\theta)^2 = \left[\frac{\lambda}{2\pi d} \sec \theta \right]^2 \left[\frac{(IQ)^2}{(I^2 + Q^2)^2} \right] \left[\frac{(\Delta I)^2}{I^2} + \frac{(\Delta Q)^2}{Q^2} - 2 \frac{(\Delta I)(\Delta Q)}{I Q} \right] \quad (5)$$

We now take the ensemble average over $(\Delta\theta)$, (ΔI) and (ΔQ) and make the reasonable assumptions that on the average:

$$I \approx Q \quad \text{and} \quad \overline{\left(\frac{\Delta I}{I}\right)^2} = \overline{\left(\frac{\Delta Q}{Q}\right)^2}$$

and $\overline{(\Delta I)(\Delta Q)} = 0$, that is the fluctuations in I and Q are uncorrelated. Then Equation (5) can be simplified to:

$$(\Delta\theta)^2 = \frac{1}{2} \left[\frac{\lambda}{2\pi d} \sec \theta \right]^2 \frac{\overline{(\Delta Q)^2}}{Q^2} \quad (6)$$

Finally we recognize the ratio $\frac{\overline{(\Delta Q)^2}}{Q^2}$ as the inverse of the signal to noise ratio (power) and write after taking the square root:

$$(\Delta\theta)_{\text{RMS}} = \frac{1}{\sqrt{2}} \left[\frac{\lambda}{2\pi d} \sec \theta \right] (\text{SNR})^{-\frac{1}{2}} \quad (7)$$

Thus, for a given operating frequency, antenna spacing and arrival angle, the root mean square fluctuation of the measured arrival angle is proportional to the reciprocal of the square root of the signal to noise ratio.

As a sample calculation, if we assume $d = 300$ m, $\lambda = 30$ m and take for a typical zenith angle $\theta = 80^\circ$ (elevation angle = 10°), then the signal to noise ratio required to achieve an RMS elevation angle error of the order of 0.1° at the probe receive site is:

$$\text{SNR} = 1.4 \times 10^3 \text{ (31 dB)}.$$

In order to achieve the same accuracy for the azimuth angle of arrival requires a SNR (where $d = 90$ m and $\theta = 0^\circ$) of 3.7×10^2 (26 dB).

With the above suggested antenna element spacing the system can meet the 0.1° requirement with a signal to noise ratio at the receiver of 30 dB. If the spacing between the antenna elements is reduced by 1/3 (an elevation antenna spacing of 100 m and an azimuthal antenna spacing of about 30 m) then the SNR requirement is increased to about 40 dB.

7.3 Signal to Noise Ratio Calculations

7.3.1 Received Signal Power

The received power over a one way path is given by:

$$P_R = \frac{P_T G_T G_R \lambda^2}{(4\pi)^2 R^2 L} \quad (8)$$

where P_T is the transmitter power, G_T is the gain of the transmitting antenna, G_R the gain of the receiving antenna, λ is the wavelength, R is the slant distance from transmitter to receiver and L is the estimated absorption losses along the propagation path. With the following set of parameters we can estimate the received power (measured in decibels relative to 1 W).

P_T	20 dBW (100 W)
G_T	10 dBi
G_R	0 dBi
f	10 MHz (night) and 20 MHz (day)
λ^2	30 dB (900 m ²) (night) and 23 dB (225 m ²) (day)
R^2	128 dB ((2400 km) ²)
L	6 dB (night) and 20 dB (day)

The resultant received power $P_R = -96$ dBW at night and -117 dBW in the daytime.

7.3.2 Noise

7.3.2.1 Atmospheric noise

The likely site for the HF probe receiving system is at Barksdale AFB, Louisiana and using this location it is possible to estimate the contribution to the output noise level from atmospheric, man-made and galactic sources using the CCIR Report #322. For the analysis in this report we have selected the fall equinox season for the hours 2000-2400 LT (night) and 0800-1200 LT (day). The CCIR tables provide the expected noise relative to $kT_0 = -204$ dBW/Hz where k is Boltzman's constant and T_0 is the standard temperature of 290° K. The atmospheric noise power is then estimated to be 51 dB/Hz above kT_0 at night (10 MHz) and 29 dB/Hz in the daytime (20 MHz), where we have added an additional 6 dB to represent the upper decile in the likely noise distribution, a correction we feel is justified on the basis of experience in finding clear channels in the HF band.

It is necessary when discussing noise power to take into account the bandwidth of the receiving system. For the probe system the selected bandwidth is 150 Hz. This then increases the noise power by 21 dB. That is, at night we can expect an atmospheric noise power level of 72 dB above kT_0B and in the daytime a noise power of 50 dB above kT_0B .

Taking into account the receiver bandwidth gives values for the atmospheric noise power of -131 dBW (for night) and -153 dBW (for day). For the above analysis of the atmospheric noise, using the CCIR #322 tables, we have assumed a specific level for the manmade contribution to the noise. Should the actual selected site at Barksdale AFB be more noisy, we should expect to have to adjust these noise power levels. Typically this should not increase by more than 10 dB with reasonable site selection.

7.3.2.2 Receiver noise

At this point we must determine the antenna preamplifier/receiver contribution to the output noise level. The goal here is to determine whether the probe system is atmospherically noise limited. The preamplifier connected directly to the 1 m monopole antenna as designed by D. M. Haines (ULCAR) has a voltage gain of 10 with a noise figure (NF) = 7 dB. Considering the transformation from the 300 Ω antenna impedance (varying with frequency) to the 950 Ω preamplifier input impedance, we estimate the input noise power to be -177 dBW. This level is well below the estimated atmospheric noise power, both day and night.

7.3.2.3 Heater transmitter leakage

ULCAR measurements have shown that if the heater frequency is more than 30 kHz above or below the probe frequency then the leakage through the 150 Hz filter is minimal and is relatively independent of the frequency separation. Considering both antenna gain and transmitter power, the heater signal is expected to be about 60 dB above the probe signal level and we considered the possibility that this could represent a significant factor in the output of the receiver even for the relatively large frequency separation of 30 kHz or more. A laboratory test was carried out to determine the effect of the high power heater signal, set 30 kHz below the probe frequency which lies within the 150 Hz band of the RACAL receiver. The two signals were injected into the RACAL from independent sources. The weaker "probe" signal was within the 150 Hz passband of the receiver and was set at a level to produce a signal to noise ratio of 30 dB while the higher level "heater" signal was 30 kHz outside the band and produced an expected signal level 60 dB above the probe signal at the input to the receiver (this was above the saturation when the receiver was tuned to the heater frequency). It was not possible to detect the effect of the out-of-band signal in the spectrum of the the receiver output and there was no change in the noise level when the "heater" signal was turned on and off.

As part of these tests, the dynamic range of the RACAL receivers was measured and found to be close to 90 dB as long as the manual gain setting was not too high (no more than half way up towards full scale). At higher gain settings the receiver seems to oscillate.

7.3.3 Signal to Noise Calculation/System Margin

Combining the results from Sections 7.3.1 and 7.3.2 to estimate the SNR that can be expected at the Barksdale AFB receive site a decision can be made as to whether the Probe system, as designed, can determine the arrival angle with the necessary precision. The following table summarizes these SNR estimates for the HF probe system. These tabulated SNR's do not include the additional improvement expected from the spectrum analysis that is used in the signal processor before the arrival angles are calculated. The additional SNR gain from the spectrum analysis is of the order of 30 dB.

<u>TIME</u>	<u>FREQUENCY</u>	<u>SIGNAL</u>	<u>NOISE</u>	<u>SNR</u>
Night	10 MHz	- 96 dB	- 131 dB	35 dB
Day	20 MHz	-117 dB	- 153 dB	36 dB

The almost constant value for the SNR results from the fact that the stronger nighttime signal power resulting from less absorption, is compensated by the increase in the noise level at night for the lower frequencies used at that time. From the above it appears that the current probe system will meet the requirements for a 0.1° arrival angle measurement capability with the proper antenna array spacing.

The only question that remains open at this time is whether the natural fluctuations in the arrival angles are significantly larger than 0.1° and effectively mask smaller changes caused by the heater modification of the local ionosphere. The answer to this problem will only be available after we get the Probe system into the field and start to gather some background data on the ionosphere's natural fluctuations.

8.0 SUMMARY

The simulation of the ionospheric depletion region has yielded results consistent with the earlier Soviet measurements and gives a certain degree of confidence to the modeling effort. These calculations show that the expected heater induced variations change in magnitude and location as the parameters of the depletion are changed. This involves focusing effects caused by the curvature in the horizontal and vertical structure of the depletion region. The results also indicate that the specific measurements, i.e. increased or decreased amplitude and the changes in the vertical angle of arrival, vary with range relative to the skip distance. The general conclusions are that the regions of maximum amplitude change and maximum elevation angle change do not coincide and multiple receive sites might be necessary to see the largest effects of both.

Given the expected order of magnitude variations in signal amplitude and arrival angles (both elevation and azimuth), the HF probe system was laid out as a three antenna interferometer with one antenna serving a dual role in both the vertical and azimuthal interferometer pairs. Since the basic design involves measuring the phase difference between the receivers, it is necessary to include into the design an automatic calibration capability to compensate for the differences between the phase characteristics in each receiver/antenna.

Using a CW transmission waveform makes it necessary to first perform a spectrum analysis on the received signal at each antenna to separate the various modes by their different Doppler shifts. The coherent dwell time for the Fourier processing was selected so that a high Doppler resolution was accomplished, sufficient to recognize the different modes which are often separated by less than 1 Hz. A nominal dwell time of twenty seconds will yield a spectrum resolution of 0.05 Hz, quite sufficient for this experiment. The sampling rate is determined by the 150 Hz bandwidth which is set by the bandpass filters of the RACAL receivers. There is no need to keep

this large bandwidth for recording, however, since most of the natural and heater induced Doppler shifts will be less than 10 Hz. The portion of the spectrum outside the region of interest (say ± 10 Hz) will therefore be simply discarded thereby greatly reducing the data storage requirements.

The three antennas are to be arranged in an "L" configuration with spacings of the order of 100 m. This can provide the required angular sensitivity if the received signal to noise ratio is sufficiently large. The estimates made here indicate somewhere between 30 to 40 dB are required depending on the selected antenna spacing. There is a clear trade-off between selected signal power and the spacing of the antenna elements. Given the proper siting for the receive system it will certainly be easier to achieve the necessary sensitivity by making the spacing larger than by trying to increase the transmitter power level by 10 dB.

The results of this modeling effort indicate that it is possible to design a HF Probe system that has the capability to detect and quantitatively measure the changes induced in the F-region of the ionosphere when sufficient heater power (90 dBW) is available.

9.0 REFERENCES

- Bochkarev, G. S., V. A. Eremenko, L. A. Lobachevsky, B. E. Ljannoy, V. V. Migulin and Yu. N. Cherkashin, "Non-linear Interaction of Decametre Radio Waves at Close Frequencies in Oblique Propagation," *J. Atmos. and Terr. Phys.*, Vol. 44, No. 12, pp. 1137-1141, 1982.
- Born, M. and E. Wolf, "Principles of Optics," *Pergamon Press*, Great Britain, 1986.
- CCIR Report 322, "World Distribution and Characteristics of Atmospheric Radio Noise," *international Telecom. Union*, Geneva, 1964.
- Field, E. C. and C. R. Warber, "Ionospheric Modification with Obliquely Incident Waves: Electron Heating and Parametric Instabilities," *RADC Final Tech. Rep.*, RADC-TR-85-188, ADA162603, 1985.
- Gurevich, A. V., "Nonlinear Phenomena in the Ionosphere," *Springer Verlag*, New York City, 1978.
- Jones, R. M. and J. J. Stephenson, "A Versatile Three-Dimensional Ray Tracing Computer Program for Radio Waves in the Ionosphere," OT Report 75-76, 1975.
- La Bahn, R. W., "Ray-Tracing in a Two-Dimensional Ionosphere," *Radio Sci.*, Vol. 20, No. 4, pp. 972-976, 1985.
- Warren, R. E., R. N. DeWitt and C. R. Warber, "A Numerical Method for using a Ray Tracing Program to Compute Radio Fields in Regions of Strong Focusing," *RADC Final Tech. Rep.*, RADC-TR-82-45, ADA113913, 1982.